

Combined Allosteric and Competitive Interaction between Extracellular Na^+ and K^+ During Ion Transport by the α_1 , α_2 , and α_3 Isoforms of the Na, K-ATPase

David M. Balshaw,* Lauren A. Millette,[†] Katherine Tepperman,[†] and Earl T. Wallick*

*Department of Pharmacology and Cell Biophysics, College of Medicine, and [†]Department of Biological Sciences, McMicken College of Arts and Sciences, University of Cincinnati, Cincinnati, Ohio 45267-0575 USA

ABSTRACT A combined allosteric and competitive model describes the interaction between extracellular Na^+ and Rb^+ during ion transport mediated by the Na, K-ATPase. The model was developed from experiments based on ^{86}Rb uptake by whole cells transfected with rat isoforms of the enzyme. In the absence of Na^+ , only a single transport site for extracellular Rb^+ exists. After the occupation of the Na^+ -specific allosteric site, the Rb^+ transport pocket opens to allow occupation by an additional Rb^+ and the subsequent transport of the two Rb^+ ions into the cells. Na^+ can also directly compete with Rb^+ for binding to at least one of the transport sites. While the model derived here applies to each of the three rat isoforms of the Na, K-ATPase expressed in HeLa cells, subtle differences exist among the isoforms. The α_3 isoform has an increased intrinsic affinity for Rb^+ and a lower affinity for the allosteric Na^+ site than α_1 or α_2 . The stimulation of uptake observed according to the best-fit model is due to the displacement by Rb^+ of inhibitory Na^+ bound to the transport site.

INTRODUCTION

The Na, K-ATPase is the plasmalemmal enzyme that catalyzes the nonequivalent transport of Na^+ and K^+ through the membrane of all animal cells. This transport activity is responsible for maintaining ion gradients and thus regulates a wide variety of cellular functions, including cardiac contractility, excitability of cells, and maintenance of osmotic balance. Under physiological conditions, the enzyme pumps three sodium ions out of the cell in exchange for the movement of two potassium ions into the cell.

The generalized reaction mechanism of the Na, K-ATPase, referred to as the Post-Albers scheme (for a review see Glynn, 1993; Lingrel and Kuntzweiler, 1994), suggests that the enzyme exists in at least two different conformations, each of which can exist in either a phosphorylated or an unphosphorylated form. These states are designated E_1 , which has a high affinity for intracellular Na^+ , and E_2 , which has a high affinity for extracellular K^+ . The cycling of the enzyme between the E_1 forms, binding cations at the intracellular face, and E_2 forms, binding cations at the extracellular face, results in the transport of the ions through the membrane.

Historically, the mechanism of transport has been analyzed by investigating the transport of radioactive ^{86}Rb , which is a congener of K^+ (Bell et al., 1977). Studies of ^{86}Rb transport have demonstrated that the overall rate-limiting step in the enzymatic cycle is the release of Rb^+ at

the intracellular surface; therefore, the studies of Rb^+ transport have focused on this step (Forbush, 1987). Recently, however, ^{86}Rb uptake has been used to study the mechanism of potassium binding and transport. Tepperman et al. (1997) analyzed the effect of low concentrations of extracellular K^+ on ^{86}Rb uptake. Although the stoichiometry was not directly measured, the model that yielded the best fit to the data was consistent with the concept that the sodium pump was capable of transporting three Na^+ for one K^+ . Plotting the displacement of ^{86}Rb uptake by nonradioactive competitor (either Rb^+ or K^+) revealed a stimulation of uptake that could be explained in terms of positive cooperativity. The displacement of uptake refers to plotting the total amount of radioactivity entering the cells without the traditional transformation into total ion transport, which masks the stimulation. This cooperativity could be rationalized as an increased affinity for the second extracellular Rb ion after the binding of the first ion. Conversely, the stimulation could be rationalized as an increase in the rate of ion flux when two Rb^+ were bound versus when only a single ion occupies the transport pocket. In this earlier study, it was not possible to distinguish between these two forms of cooperativity. If, however, the concentrations of radioactive and nonradioactive Rb^+ are independently varied, the data fit models that suggest that both forms of cooperativity exist, in different proportions for each of the three major isoforms of the catalytic subunit (Balshaw and Wallick, unpublished observations).

Extracellular Na^+ is known to act as a low-affinity competitive inhibitor of K^+ binding at the extracellular surface (Sachs, 1977). In addition to the competitive interaction between Na^+ and K^+ at both the intracellular and extracellular ion binding sites, extracellular Na^+ has been implicated as an allosteric effector of K^+ uptake. The hypothesis that external Na^+ has an allosteric effect initially came from Cavieres, who proposed that Na^+ acts only as an allosteric

Received for publication 18 February 1999 and in final form 13 April 2000.

Address reprint requests to Dr. David Balshaw, Department of Biochemistry and Biophysics, University of North Carolina, Chapel Hill, NC 27599. Tel.: 919-966-5021; Fax: 919-966-2852; E-mail: balshaw@med.unc.edu. Dr. Millette's present address is Astra Pharmaceuticals, 325 Kaw Lane East, Lake Quivira, KS 66217.

© 2000 by the Biophysical Society

0006-3495/00/08/853/10 \$2.00

inhibitor of K^+ activation (Cavieres and Glynn, 1979). Sachs refined this hypothesis by showing that a simple allosteric model was incapable of describing the data for K^+ and Cs^+ transport; likewise, a simple competitive model did not adequately describe the data. To fit the data a combined model encompassing both allosteric and competitive inhibition was required (Sachs, 1977). Despite these studies, the effects of external Na^+ on ion transport are not fully understood.

The experiments described here tested the effect of external Na^+ on the function of the Na^+ , K^+ -ATPase. A model is developed that provides the best fit to the data, consistent with a dual role for Na^+ , including both allosteric and competitive interactions. The importance of this work is the details it adds about both the competitive and allosteric interactions of external Na^+ and how these affect the transport of K^+ .

EXPERIMENTAL PROCEDURES

Cell culture

HeLa cells expressing the rat α_1 isoform were the gift of Dr. Lois Lane. HeLa cells expressing the rat α_2^* or rat α_3^* were the gift of Dr. Jerry Lingrel. The asterisk denotes mutation of the amino acids bordering the H1H2 transmembrane domain to charged residues, decreasing the affinity for ouabain by 1000-fold (Price et al., 1989). Cells were maintained in Dulbecco's minimum essential medium with 1 μ M ouabain as described previously (Tepperman et al., 1997). Supplies for cell culture and general laboratory chemicals were purchased from Gibco (Grand Island, NY), Life Technologies (Rockville, MD), Sigma (St. Louis, MO), or Fisher Scientific (Pittsburgh, PA).

^{86}Rb uptake assay

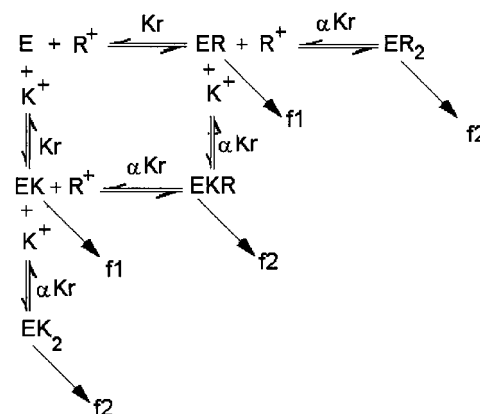
The experiments analyzing the interaction between extracellular Na^+ and Rb^+ at the extracellular site were carried out essentially as previously described (Tepperman et al.). Briefly, stably transfected HeLa cells were plated in 24-well tissue culture plates at 3×10^4 cells per well and were grown to ~80% confluency. Cells were rinsed and then preincubated for 30 min with a solution containing zero Na^+ /zero K^+ Tris- P_i (15 mM Tris PO_4 , pH 7.4, 135 mM choline chloride, 5 mM glucose, 0.5 mM $MgCl_2$, 0.5 mM $CaCl_2$). The solution also contained 1 μ M ouabain and 1 mM furosemide. The cells were then changed to prewarmed solutions containing variations in both the NaCl (12 concentrations) and nonradioactive RbCl (12 concentrations) in Tris- P_i buffer, with choline chloride used to maintain the ionic strength (a total of 144 combinations of Na^+ and Rb^+). All samples were exposed to the same concentration of carrier free $^{86}RbCl$ (Dupont NEN, Boston, MA), typically 1–10 μ M, for 10 min at 37°C. All experiments were performed in duplicate. The incubation was stopped by the

addition of ice-cold zero Na^+ /zero K^+ Tris buffer and rinsed eight times in this solution. The cells were treated with 0.5 ml of 0.2 N NaOH for 1 h and neutralized with HCl. The total contents of each well were then transferred to a scintillation vial and then counted.

Data analysis

The data were plotted as mean \pm standard error and were typically plotted as a nonradioactive RbCl displacement at a single concentration of extracellular NaCl. These individual Rb^+ displacements were fit to Eq. 1 (described by Tepperman et al. (1997)) or to a four-parameter logistic function, using the commercial program Kaleidagraph (Synergy Software), which uses the Marquardt-Levenberg algorithm for minimization of weighted least squares. Model 1, shown below, is the ordered binding model used previously (Tepperman et al., 1997) that describes the stimulation of uptake by low concentrations of competitor. The mathematical equation describing the uptake of radioactive Rb^+ , derived from model 1, is given below, where R represents the concentration of radioactive Rb^+ and K represents the non-radioactive Rb^+ :

$$U = U_{\max}^* \left(\frac{\left(\frac{R}{K_r^*} \right) + \left(\frac{2R^2 + (R^*K)}{\alpha^* K_r^2} \right)}{2^* \left(1 + \left(\frac{R + K}{K_r} \right) + \left(\frac{R^2 + (R^*K) + K^2}{\alpha^* K_r^2} \right) \right)} \right) + NS^*R \quad (1)$$



Model 1. Ordered model for displacement of radioactive Rb (R) by nonradioactive Rb (K). R symbolizes radioactive ^{86}Rb and K nonradioactive ^{85}Rb . K_r is the apparent dissociation constant for the binding of the first Rb^+ ion, and α is the interaction coefficient, describing the change in dissociation constant for binding of the second ion. When the enzyme has the binding pocket occupied by only a single ion, Rb^+ is transported into the cell with an apparent first-order rate constant, f_1 . This rate constant is a combined constant describing all of the processes from the binding of Rb^+ through transport and the exposure of the binding pocket at the extracellular site. When the binding pocket has a second ion present, this combined rate constant becomes f_2 .

The term f in the equation is the ratio f_2/f_1 . The maximum uptake, U_{\max} , is defined as the amount of uptake that would occur at saturating concentrations of ^{86}Rb and is determined by the curve fitting process. The nonspecific uptake, NS, is the amount of radioactivity associated with the cells that cannot be competed out by infinite concentrations of nonradioactive competitor. The model and equation shown are for ordered (or sequential) uptake of $^{86}\text{Rb}^+$. We use the term "ordered" to mean that there is a single binding pocket in which one or two cations can bind. However, a random model in which there are two distinct, noninteracting sites for K^+ fits equally well. The random model has one additional binding constant.

The combined data for a given experiment (144 concentrations of extracellular Na^+ and Rb^+) were analyzed with SigmaPlot (version 5.01 for Macintosh or DOS PC; Jandel Scientific (now SPSS), Chicago, IL), using shared parameters between curves fit to models described in the Results and Discussion sections. SigmaPlot uses the Marquardt-Levenberg algorithm for minimization of weighted least squares. The parameters describing the affinity of a binding site were assumed to be log-normally distributed (cannot equal or be less than 0) and were defined in the curve-fitting algorithm accordingly, i.e., $K_r = 10^{\log(K_r)}$. For all curve fits, the existence of local minima in the error space of the fit parameters was determined by varying the initial estimates. The ability to adequately resolve the parameters for a given model was determined by first simulating data, incorporating random error, and fitting these simulated data to the model.

The weighting scheme was determined experimentally. The initial approximation was that our data had a constant percentage error and the data were weighted to the theoretical standard deviation (TSD) by the relationship

$$\text{TSD} = (\text{mean} * c) \quad (2)$$

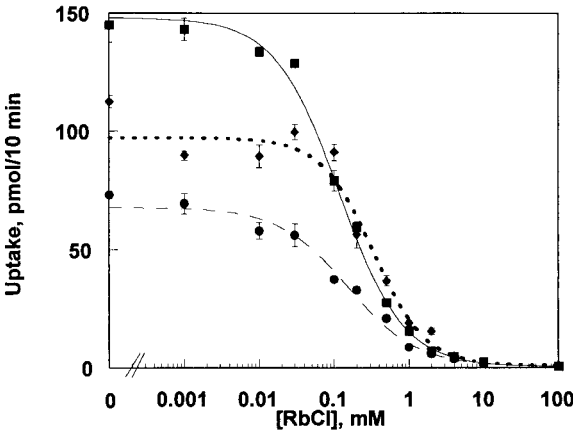


FIGURE 1 Rb displacement of uptake in the absence of extracellular Na^+ . ^{86}Rb uptake in 10 min is plotted as a function of the concentration of nonradioactive RbCl for the three isoforms of the Na, K-ATPase (α_1 , —■—; α_2^* , - -◆- -; α_3^* , ●●●). Curves are fits to the four-parameter logistic function.

TABLE 1 Rb⁺ displacement in the absence of Na^+

Isoform (<i>n</i>)	IC_{50} (mM)	n_i
Rat α_1 (4)	0.123 ± 0.011	0.972 ± 0.035
Rat α_2^* (4)	0.105 ± 0.014	0.829 ± 0.049
Rat α_3^* (4)	$0.055 \pm 0.019^{\dagger\dagger}$	0.783 ± 0.070

$^{\dagger}p < 0.05$ in comparison with Rat α_1 .
 $^{\dagger\dagger}p < 0.05$ in comparison with Rat α_2^* , using a Fisher's PSLD post hoc analysis.
 Values are means \pm standard error.

where c is the constant percentage error, measured to be 0.113. The data were weighted to $1/\text{TSD}^2$. The predicted correlation between the mean of the replicates and the standard deviation was confirmed in this study (data not shown). Goodness of fit was analyzed in terms of the number of runs (change in sign of the residuals), χ^2 (sum of the squares of the weighted residuals), dependencies between parameters (effect of altering the other parameters on a given parameter), and the parameter errors. The statistical significance of differences between parameter values for each isoform was determined by application of a one-way analysis of variance with post hoc use of Fisher's Protected Least Significant Difference test to the parameter results for all experiments for the isoforms being compared, using StatView version 4.5 (Abacus Software, Berkeley, CA).

RESULTS

Displacement of ^{86}Rb uptake by nonradioactive Rb^+ in the absence of extracellular Na^+

Fig. 1 shows the inhibition of ^{86}Rb uptake in the absence of extracellular Na^+ by nonradioactive Rb^+ for the α_1 , α_2^* , and α_3^* isoforms. The data are shown fit to a four-param-

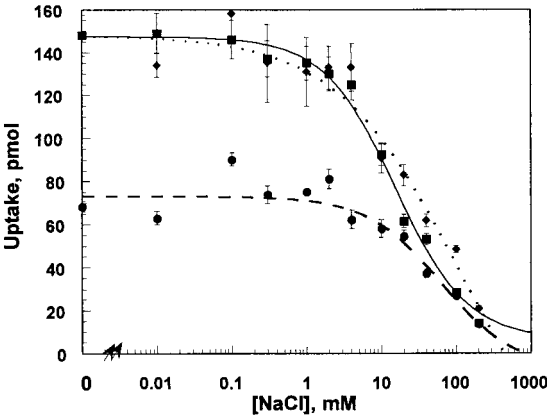


FIGURE 2 Na displacement in the absence of added nonradioactive Rb^+ . Data are fit to the four-parameter logistic function. Symbols are defined in the legend for Fig. 1.

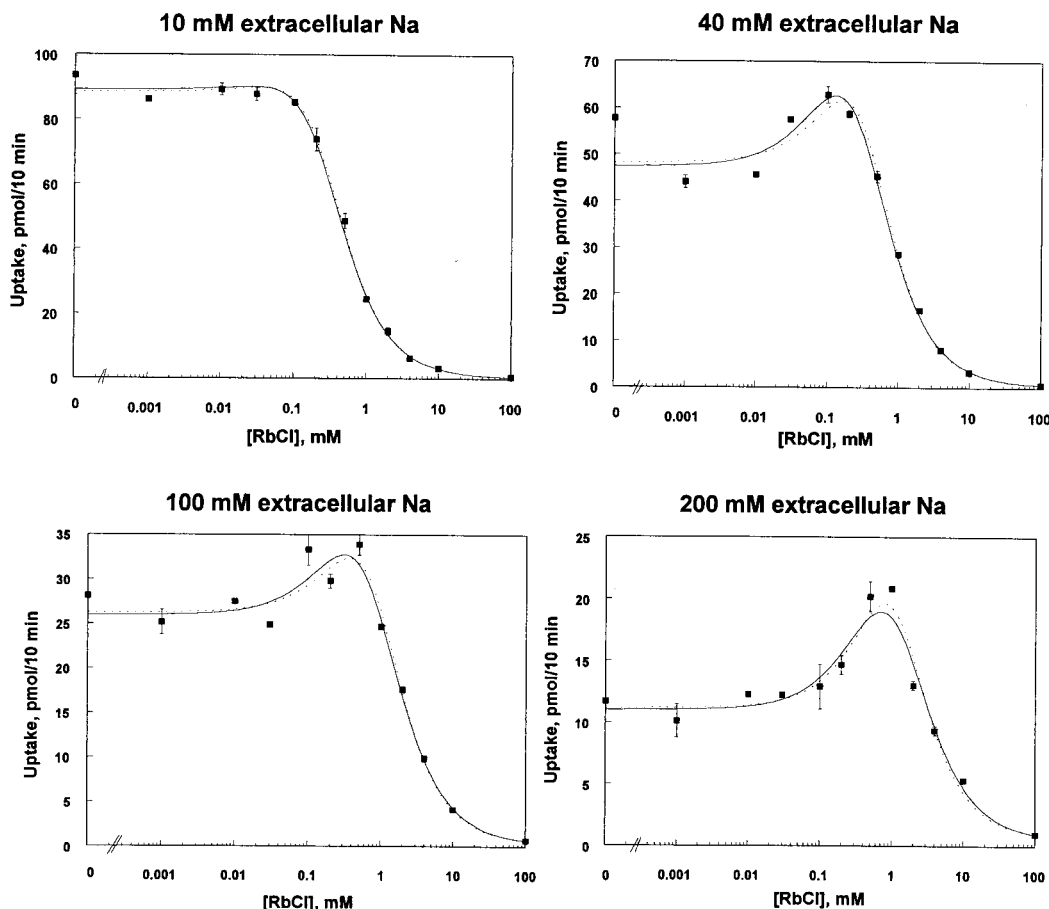


FIGURE 3 Effect of Na^+ on the displacement of ^{86}Rb uptake by RbCl . Rb^+ displacements of uptake were performed at different concentrations of extracellular NaCl , given in the panel title. The data are fit to the ordered binding (model 1), with cooperativity in either flux rate (.....) or binding affinity (—).

eter logistic function (Eq. 3),

$$Y = \left(\frac{\max - \min}{1 + \left(\frac{X}{\text{IC}_{50}} \right)^{n_i}} \right) + \min \quad (3)$$

This function describes the maximum level of uptake, max; the minimum level of uptake, min; the concentration of ligand that makes the value of Y (in this instance, uptake of $^{86}\text{Rb}^+$) half of the distance between max and min, IC_{50} ; and a slope factor at the IC_{50} value, n_i . The data for fits to the four-parameter logistic function for the three isoforms are summarized in Table 1. For the α_1 and α_2^* isoforms the values of IC_{50} in the absence of Na^+ , which approximates the intrinsic affinity for Rb^+ , are nearly identical, whereas the affinity for the α_3^* isoform (0.055 mM) is twofold greater than those for α_1 (0.123 mM) and α_2^* (0.105 mM). Furthermore, all three isoforms have nearly identical values for n_i that are not significantly different from 1, indicating that in the absence of external Na^+ there exists only a single site for the transport of Rb^+ .

Na^+ displacement of ^{86}Rb uptake in minimal extracellular Rb

The corollary graphs, plotting the displacement by Na^+ of ^{86}Rb uptake in the absence of added nonradioactive Rb^+ (total $[\text{Rb}^+] \sim 10 \mu\text{M}$), are shown in Fig. 2. The fact that Na^+ decreases the amount of uptake suggests that Na^+ acts as an inhibitor of ^{86}Rb uptake, albeit requiring higher concentrations than the displacement by nonradioactive Rb^+ . These data indicate that the three isoforms have nearly identical interactions with competitive Na^+ .

Effect of external Na^+ on nonradioactive Rb^+ displacement of ^{86}Rb uptake

Rb^+ displacement assays (12 concentrations of nonradioactive Rb^+) were performed at 12 concentrations of extracellular Na^+ on paired plates. These experiments were performed on the same day with cells that were plated on the same day at the same density. A representative series of the

plots of the data sets obtained in this manner were fit (model 1) to the cooperativity in flux model (Eq. 1, $\alpha = 1$) and the cooperativity in binding model (Eq. 1, $f = 1$) and are shown in Fig. 3 for the rat α_1 isoform. The rat α_2^* and rat α_3^* isoforms showed similar results. At low concentrations of extracellular Na^+ (less than 10 mM) there is no apparent stimulation of uptake by nonradioactive Rb^+ (Fig. 3 A). The Hill coefficient is close to 1, indicating the presence of a single site, as observed in the absence of Na^+ (Fig. 1). In contrast, at concentrations higher than 10 mM external Na^+ , stimulation appears and is maintained up to 200 mM (Fig. 3, B–D). As suggested earlier (Tepperman et al., 1997), the stimulation can be accounted for by cooperativity either in binding or in flux. Both of these models describing the stimulation of uptake, which apply only at concentrations above 10 mM Na^+ , require that there be two sites for external Rb^+ .

Models that assume a simple competitive effect of Na^+

Based on Fig. 2, external Na^+ clearly inhibits the uptake of radioactive Rb^+ . We first considered a simple model in which Na^+ and Rb^+ compete. Because in the absence of Na^+ there was only a single site for Rb^+ , a single-site model with one external site to which either Na^+ or Rb^+ could bind was tested. Thus the only species present are E, ER, and EN. Only ER can translocate Rb^+ . This model will not show stimulation at any concentration of Na^+ or Rb^+ , because only a single ion is transported, and fits to the combined data at 12 Na^+ and 12 Rb^+ concentrations failed to converge for the rat α_1 and rat α_2^* isoforms. The fit did converge with data for the rat α_3^* ; however, the fit statistics were very poor, with a χ^2 value of 1300 (144 data points).

Another model was used, in which Na^+ acts as a simple competitor for ^{86}Rb uptake and in which there are two Rb^+ binding sites. This model is the same as the ordered binding model (model 1), with the addition of Na^+ as a competitor for the binding of the first Rb^+ . Thus the only species that exist are E, ER, ER_2 , and EN. This model will always show stimulation of uptake by Rb^+ , regardless of sodium concentration. Fits of the data to this model failed to converge with any of the isoforms or converged with a large error in the parameters and high χ^2 values.

Assumption of a combined competitive and allosteric effect of Na^+

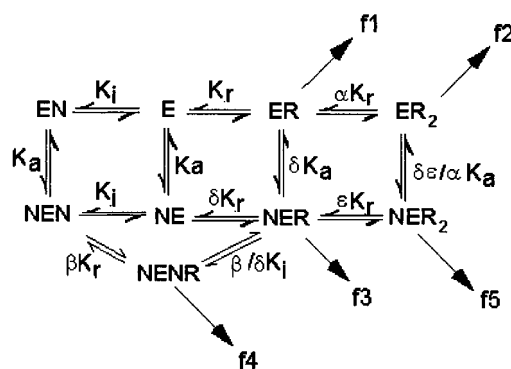
Treating external Na^+ as a simple competitor of Rb^+ transport was not adequate to explain the data. Based on Figs. 1 and 3, it is clear that the mechanism of transport changes from a single Rb^+ site at low Na^+ to two Rb^+ sites at higher Na^+ , suggesting that external Na^+ is having an allosteric effect as well as a competitive effect. Consistent with this,

the U_{max} derived from fits to data for all three isoforms shows that U_{max} increases with increasing external Na^+ .

Model 1 is shown, with R representing radioactive Rb^+ and K representing nonradioactive displacing Rb^+ . To simplify the presentation, the remaining models are shown as binding models containing only radioactive tracer and can be converted to the displacement scheme by the addition of enzyme species with K representing nonradioactive Rb^+ as in model 1. Model 1 has been expanded to include the mixed allosteric and competitive interaction between Na^+ and Rb^+ (see model 2 below).

In model 2 the potassium transport site is capable of binding either Rb^+ or a competitive Na^+ . Once the transport site is occupied by the first ion (binding constant K_r , transport rate f_1), the affinity for the second ion is influenced by a factor, α , and both ions are transported at the rate f_2 . Occupation of the allosteric site by Na^+ alters the binding constant for the first ion in the transport pocket by the factor δ (transport rate f_3) and the second ion by the factor ϵ (transport rate f_5). In addition, in model 2 the enzyme with the allosteric site occupied is capable of binding both Rb^+ and Na^+ in the transport pocket simultaneously (species NENR), with the binding constant being altered by the factor β and transport occurring at the rate f_4 . A displacement scheme based upon model 2 would include additional species for nonradioactive competitor (EK, EK_2 , NEK, NEK_2 , NENK, ERK, NERK). Likewise, the equation used for fitting the data (not shown) contains additional terms for the nonradioactive competitor.

As with model 1, it is impossible to distinguish between the two forms of cooperativity (binding affinity and flux



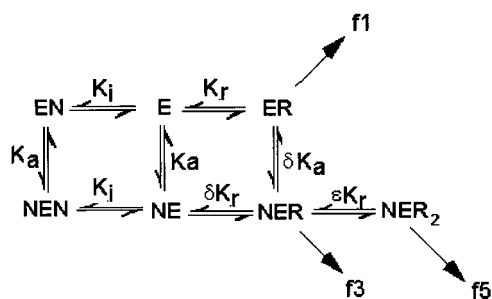
Model 2. General model for a combined allosteric and competitive effect of external Na^+ . R represents Rb and N sodium. EN represents binding of Na^+ to the transport site and NE represents binding of Na^+ to the allosteric site. K_r is the constant for the binding of the first Rb^+ to the K transport site, K_i is the constant for binding of Na^+ to the K transport site, and K_a is the constant for the binding of Na^+ to the allosteric site. α , β , δ , and ϵ are interaction coefficients reflecting the effect of previously bound ion(s) on the subsequent binding of an additional ion. f_1 through f_5 represent the flux constants for the indicated species. These are combined rate constants describing all of the steps in the enzyme cycle downstream of the binding event at the extracellular surface through the reopening of the potassium binding pocket at the extracellular surface.

rate) at a single concentration of ^{86}Rb . This necessitates the assumption that only one form of cooperativity exists. If it is assumed that all of the transport is due to an increased flux rate ($\alpha = \beta = \delta = \epsilon = 1$) or increased affinity ($f_1 = f_2 = f_3 = f_4 = f_5$), transport through the species NER_2 is assumed to be fastest with the rate f_5 . U_{\max} , therefore, is defined as the transport occurring when all of the enzyme has the allosteric site occupied and two ^{86}Rb ions bound; mathematically, $U_{\max} = 2f_5[E_{\text{tot}}]$.

Simultaneous fits to models 2 and 3

Attempts to simultaneously fit data from experiments using 12 concentrations each of external Na^+ and nonradioactive Rb^+ to model 2, the more general, failed to converge or converged with large parameter errors. Because Fig. 1 showed that only a single Rb^+ site exists in the absence of Na^+ , species ER_2 was eliminated, improving the frequency of convergence. The coefficient matrix, however, was singular, indicating that one or more parameters had no influence on the shape of the curve. This parameter was the term describing the NENR species, which had a value that was either extremely large for β or small for f_{45} , indicating that, if this species does exist, it plays no role in transporting ions. Eliminating ER_2 and NENR led to model 3, which yielded the best fits.

In best fit model 3, the potassium transport pocket is able to bind either a Rb^+ ion or a competitive Na^+ . If a Rb^+ is bound, it will transport with a rate f_1 . Occupation of the allosteric site by Na^+ alters the binding constant of the transport pocket for the first ion by the factor δ and the second by the factor ϵ . These ions are then transported at the rates f_3 and f_5 , respectively. A displacement scheme based upon model 3 would include additional species for nonradioactive competitor (EK, NEK, NEK_2 , NERK). Equation 4 describes the uptake of radioactive Rb^+ in the presence of nonradioactive Rb^+ :



Model 3. Best fit model. Symbols are as defined in model 2.

$$U = U_{\max}^* \left(\frac{\left(\frac{R}{f_{51}K_r} + \frac{NR}{f_{53}\delta K_r K_a} + \frac{N(2R^2 + (RK))}{\delta \epsilon K_r^2 K_a} \right)}{2 \left(1 + \frac{R + K}{K_r} + \frac{N(R + K)}{\delta K_r K_a} \right) + \frac{N(R^2 + (RK) + K^2)}{\delta \epsilon K_r^2 K_a} + \frac{N}{K_a} + \frac{N}{K_i} + \frac{N^2}{K_i K_a} \right)} + \text{NS}^* R \quad (4)$$

The term f_{51} in the equation is the ratio f_5/f_1 , and f_{53} is the ratio f_5/f_3 . The maximum uptake, U_{\max} , is defined as the amount of uptake that would occur at saturating concentrations of ^{86}Rb and is determined by the curve-fitting process. The nonspecific (NS) uptake is the amount of radioactivity that is associated with the cells and cannot be competed out by infinite concentrations of nonradioactive competitor. As with models 1 and 2, it is impossible to distinguish between the two possible forms of cooperativity (in binding or flux rate). This necessitates the assumption that only one form of cooperativity exists. If it is assumed that $f_1 = f_3 = f_5$, the ratios f_{51} and f_{53} are equal to 1. These are referred to as affinity fits (Fig. 4 and Table 2). If it is assumed that all of the affinities are the same (δ and $\epsilon = 1$), these are referred to as flux fits (Fig. 5 and Table 3).

The results of these simultaneous fits show that the α_3^* isoform has a higher affinity for Rb^+ than either the α_1 or α_2^* isoforms and that the affinities for the competitive Na^+ specific sites, K_i , are not significantly different for the three isoforms. The affinity for the allosteric site in the rat α_3^* isoform has a large error because it is poorly resolved; nonetheless, the value for K_a in rat α_3^* is significantly decreased in comparison to both the rat α_1 and rat α_2^* in both models.

An additional model tested was a random model in which binding Na^+ to the allosteric site opens a second, independent potassium-binding site. This allows for the existence of two species of NEK as opposed to one species for the ordered model. It was expected that this model would be able to describe the data as well as the ordered model discussed above; however, it failed to converge for any of the isoforms without a large error. Presumably this error is due to the high degree of dependence between the values of the two binding constants for the second Rb ion after the binding of allosteric Na^+ . A final model tested was one that allowed an allosteric activation of uptake by Na^+ without competitive inhibition by Na^+ . This model did converge with each of the isoforms, but the χ^2 were poor, averaging ~ 2000 , as compared to 300–800 (144 data points), for the fits to the combined model. Of seven models tested, model 3 best describes the interactions of external Na^+ and K^+ ions with the Na, K-ATPase.

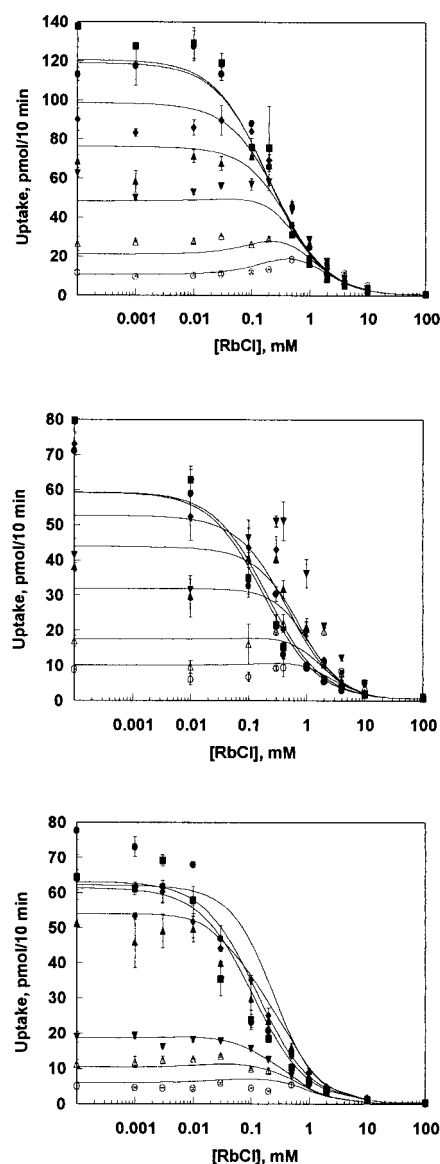


FIGURE 4 Na⁺, K⁺ interaction assuming cooperativity in binding affinity only. Data for model 3 assuming cooperativity in binding affinity. This assumption was made by fixing $f_{51} = f_{53} = 1$. The data points are mean \pm standard error for a single experiment performed in duplicate. The fit results are K_r , K_i , K_a (mM), δ , ϵ (unitless), U_{max} (pmol/10 min), NS (pmol/10 min μ M 86 Rb), and χ^2 : for rat α_1 (top), 0.189 ± 0.010 ; 25.5 ± 11.9 , 23.3 ± 14.1 , 1.60 ± 1.04 , 0.911 ± 0.324 , $(4.04 \pm 0.13) \cdot 10^4$, 409 ± 36 , 339; for rat α_2^* (middle), 0.173 ± 0.019 , 18.4 ± 10.0 , 14.0 ± 9.2 , 0.540 ± 0.290 , 5.00 ± 3.20 , $(1.78 \pm 0.11) \cdot 10^3$, 53.6 ± 4.5 , 400; and for rat α_3^* (bottom), 0.102 ± 0.009 , 12.3 ± 2.1 , 23.9 ± 14.1 , 0.266 ± 0.480 , 4.44 ± 0.77 , $(2.43 \pm 0.14) \cdot 10^3$, 89.7 ± 6.8 , 640. The plots shown give seven of a total of 12 concentrations of Na⁺. Not shown are 0.01, 0.1, 0.3, 2, and 4 mM. ■, 0 mM Na; ●, 1 mM; ◆, 10 mM; ▲, 20 mM; ▼, 40 mM; △, 100 mM; ○, 200 mM.

DISCUSSION

Of the models tested, model 3 gave the best fit to the data, with χ^2 ranging from 433 to 882 (expected $\chi^2 \sim 140$). The

errors in the parameters were not unreasonable. It is probable that the errors in the description of the data by the combined fits are due to the complexity of the model. We know, for example (unpublished data), that there is cooperativity in both flux and affinity.

The results of combined fits, whether to a cooperative in affinity-only model or a cooperative in flux-only model, show that the K_r for Rb⁺ binding to the transport site ranges from 0.1 to 0.2 mM, with α_3 having significantly higher affinity than either α_1 or α_2 . The K_i for Na⁺ binding to the transport site was 33–114-fold higher. The K_a for Na⁺ binding to the allosteric site varied widely from 9.8 mM to 51 mM, with α_3 having significantly lower affinity than either α_1 or α_2 . For all three isoforms, binding of Na⁺ to the allosteric site increases the affinity of the enzyme for K⁺ by threefold, as indicated by the value of δ (Table 2). Alternatively, the total flux is increased by fourfold by the occupation of the allosteric site, twofold by the increase in f_{51} (Table 3), and twofold for two Rb ions being transported rather than one when the allosteric site is unoccupied.

The values for ϵ or f_{53} indicate negative cooperativity, i.e., ϵ greater than δ or f_{51} less than 1 (Tables 2 and 3). While our previous work at 150 mM external Na⁺ suggested that the observed stimulation of 86 Rb uptake was due to positive cooperativity, the model (model 1) used did not include either the allosteric site or the competitive site for Na⁺ (Tepperman et al., 1997). Adding a competitive site for Na⁺ to model 1, as shown by simulations, indicated that stimulation of uptake could occur whether there was positive or negative cooperativity or no cooperativity. Addition of the allosteric site gave the same results. With our present best-fit model (model 3), at saturating Na⁺ and low concentrations of K⁺ (nonradioactive Rb⁺), transport is due only to the species NER. As K⁺ increases, the additional transporting species NEKR appears as Na⁺ in the competitive site is displaced by nonradioactive Rb⁺. The stimulation of uptake observed is due almost entirely to the rise in this species. As K⁺ increases further, radioactive Rb uptake decreases because the R in NEKR is displaced by K (NEKK).

When we compare the different isoforms, whether analyzed by the cooperativity in binding only model or the cooperativity in flux only model, the value for K_r indicates that α_3^* has a higher affinity for Rb⁺ binding to the transport site and a lower affinity for Na⁺ binding to the allosteric site than the other isoforms. The values for K_i indicate that all isoforms have a similar affinity for Na⁺ binding to the transport site. The resolution of the affinity fits for the allosteric site is quite poor for the α_3^* isoform, presumably because of its lower affinity, and therefore, the data do not reveal the shape of the curve at high Na⁺ relative to K_a . This poor resolution, in turn, decreases the resolution of the parameters describing the cooperativity factor ϵ . Analyzing the data according to model 3 indicates that the α_3^* isoform has either a decreased affinity for the allosteric site or a decrease in the overall cooperativity, resulting in a decrease

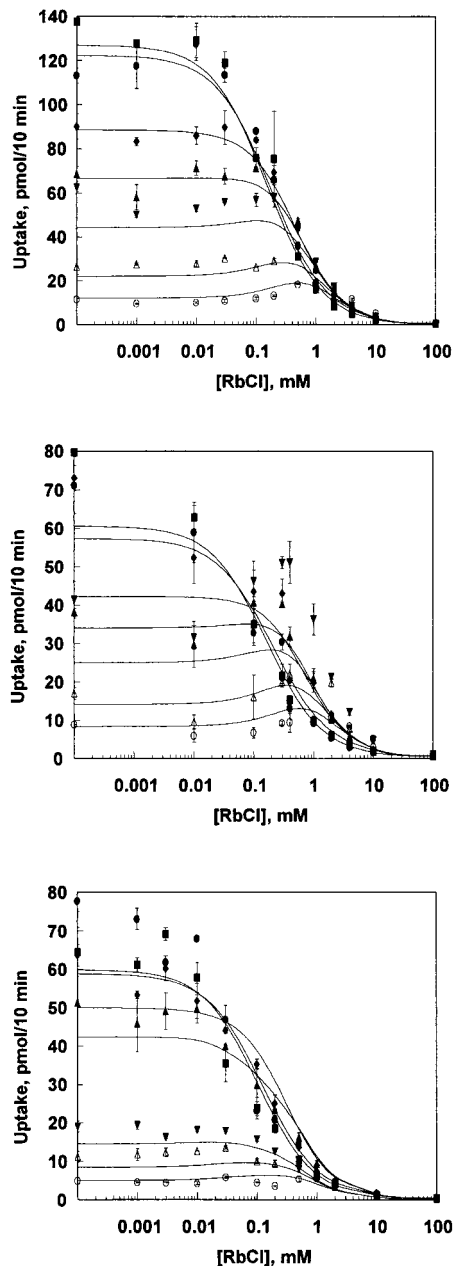


FIGURE 5 Na^+ , K^+ interaction assuming cooperativity in flux rate only. Data were fit to the combined model 3, assuming that all of the cooperativity is due to an increased flux rate. The data points are mean \pm standard error for a single experiment performed in duplicate. The fit results are K_t , K_i , K_a (mM), f_{51} , f_{53} (unitless), U_{\max} (pmol/10 min), NS (pmol/10 min μM ^{86}Rb), and χ^2 : for rat α_1 (top), 0.150 ± 0.010 , 6.61 ± 1.75 , 23.3 ± 14.1 , 1.36 ± 0.08 , 0.451 ± 0.138 , $(4.64 \pm 0.21) \times 10^4$, 389 ± 33 , 266; for rat α_2^* (middle), 0.152 ± 0.018 , 5.49 ± 2.65 , 38.8 ± 11.6 , 1.90 ± 0.20 , 0.385 ± 0.235 , $(3.09 \pm 0.26) \times 10^3$, 48.1 ± 4.4 , 369; and for rat α_3^* (bottom), 0.098 ± 0.011 , 7.33 ± 3.06 , 42.5 ± 11.8 , 1.32 ± 0.17 , 0.235 ± 0.121 , $(3.03 \pm 0.31) \times 10^3$, 85.9 ± 6.3 , 524. The plots shown give seven of a total of 12 concentrations of Na^+ . Not shown are 0.01, 0.1, 0.3, 2, and 4 mM. Symbols are as in Fig. 4.

in the stimulation observed in the maximum allowable Na^+ concentration of 200 mM.

Data from the literature analyzed by Hill plots or by Dixon plots suggest a complex interaction of Na^+ , K^+ -ATPase with external Na^+ . For example, in the presence of 150 mM external Na^+ , activation of the pump current by extracellular K^+ was found to have a Hill coefficient of 1.5 for the rat α_2^* isoform (Yamamoto et al., 1996). Neither the IC_{50} nor the Hill coefficient for extracellular K^+ was altered by the concentration of intracellular Na^+ . It was recognized quite early (Skou, 1957; Squires, 1965; Sachs and Welt, 1967) that a plot of enzyme ATPase activity against external K^+ yielded a sigmoidal curve (suggesting at least two sites) in the presence of a high, fixed Na^+ concentration. Similarly, a plot of ouabain-sensitive K^+ influx in human red blood cells as a function of external K^+ is sigmoidal if the measurements are made in high Na^+ solution. In contrast, when the influx measurements are made in Na^+ -free solutions, the curve is almost hyperbolic (suggesting a single site) (Sachs, 1967; Garrahan and Glynn, 1967; Priestland and Whittam, 1968). Dixon plots ($1/v$ versus Na^+) are nonlinear at low K^+ but become linear at higher K^+ (Cavieres and Ellory, 1975).

To explain the experimental observations, Cavieres proposed that Na^+ acts as an allosteric inhibitor of the pump (Cavieres and Ellory, 1975). This model assumes that K^+ binds to the extracellular surface at two sites, one with a high affinity and the other with a lower affinity. This model requires that both transport sites be occupied for transport of K^+ to occur. The action of the allosteric Na^+ was proposed to further decrease the affinity of the lower affinity site, thereby decreasing the transport. While this model partially rationalizes the downward curve of Dixon plots at low K^+ , it predicts that these curves will be nonlinear at all K^+ concentrations, which they are not. This model, therefore, does not account for the Hill coefficient of 1 in the absence of Na^+ . Furthermore, the fundamental assumption that both K^+ ions must be bound before transport occurs is inconsistent with the findings of Forbush (1988) and the model presented by Tepperman et al. (1997).

Sachs (1977) extended Cavieres' study by including a competitive inhibition by Na^+ of ^{86}Rb and ^{137}Cs uptake as well as a heterotropic allosteric effector site for Na^+ ; Sachs' model also allowed for transport when only a single ion is bound. This random binding model predicts that, in the absence of extracellular Na^+ , the K^+ activation of the curve will be hyperbolic and correctly predicts the curvature of Dixon plots at low K^+ and the linearity at higher concentrations. Because of the number of parameters in the model, Sachs was forced to make the assumption that the occupation of the allosteric site increased the affinity for both the first and second sites equally and fixed the parameters for the affinity for the first and second K^+ ions and V_{\max} from a single plot in the absence of Na^+ . While this study was heroic and is the best rationalization to date of the interac-

TABLE 2 Results of combined fits: cooperativity in affinity-only model

Isoform (<i>n</i>)	K_r (mM)	K_i (mM)	K_a (mM)	δ	ε	χ^2
Rat α_1 (4)	0.200 ± 0.021	9.98 ± 2.98	15.5 ± 2.4	0.381 ± 0.187	1.13 ± 0.06	631 ± 117
Rat α_2^* (4)	0.233 ± 0.018	7.71 ± 1.05	9.81 ± 4.02	0.317 ± .052	0.958 ± 0.236	861 ± 53
Rat α_3^* (4)	0.125 ± 0.019 ^{†‡}	14.3 ± 5.2	50.8 ± 13.6 ^{†‡}	0.329 ± 0.106	2.88 ± 0.771	882 ± 114

[†] $p < 0.05$ in comparison with Rat α_1 .

[‡] $p < 0.05$ in comparison with Rat α_2^* , using a Fisher's PSLD post hoc analysis.

Values are means ± standard error.

TABLE 3 Results of combined fits: cooperativity in flux rate-only model

Isoform (<i>n</i>)	K_r (mM)	K_i (mM)	K_a (mM)	f_{51}	f_{53}	χ^2
Rat α_1 (4)	0.128 ± 0.007	5.48 ± 0.62	26.1 ± 3.7	1.70 ± 0.19	0.310 ± 0.025	433 ± 68
Rat α_2^* (4)	0.157 ± 0.004 [†]	5.36 ± 0.38	33.3 ± 7.3	1.99 ± 0.07	0.339 ± 0.036	610 ± 27
Rat α_3^* (4)	0.092 ± 0.004 ^{†‡}	7.54 ± 1.01	139 ± 34 ^{†‡}	1.74 ± 0.16	0.178 ± 0.031 ^{†‡}	647 ± 51

[†] $p < 0.05$ in comparison with Rat α_1 .

[‡] $p < 0.05$ in comparison with Rat α_2^* , using a Fisher's PSLD post hoc analysis.

Values are means ± standard error.

tion between Na⁺ and K⁺ at the extracellular surface, the χ^2 value for the fit was 952 for 60 data points, which, according to the maximum likelihood theory estimation (Press et al., 1986), did not adequately describe the data. The curve fit is particularly poor at describing Sachs' data at high Na⁺ and K⁺. This combined allosteric and competitive interaction scheme of Sachs, however, was a better model than either the competitive or allosteric interaction alone, the fits of which χ^2 of ~6000. Maximum likelihood theory estimation says that the fit of our data to our combined allosteric-competitive model is not perfect but is an improvement over the fits shown by Sachs.

Our data are not consistent with transport models requiring the transport pocket to be filled with two cations before transport can occur. Our data are consistent with models that show a change in mechanism when the external Na⁺ concentration is changed from zero (one Rb⁺ being transported) to higher values (two Rb⁺ being transported). Our data are more consistent with a combined allosteric-competitive model than with an allosteric only or a competitive only model. Our conclusions and the model are applicable for external Na⁺ concentrations from zero to 200 mM and external K⁺ concentrations from 10 μ M to 100 mM.

The physiological effect of the subtle differences in the ion sensitivity and cooperativity in the three isoforms in normal adults (Na = 140 mM, K = 4.1 mM; Lentner, 1984) is not great, because 93% of the enzyme for α_1 and α_2 would be transporting via the species NEKK. For α_3 this drops to 90%. In hypernatremic (200 mM Na⁺) and hyponatremic (90 mM Na⁺) disease states, these fractions are not significantly changed. In hyperkalemic (10 mM) disease states, the ratios for the three isoforms are 97% for α_1 and α_2 and 96% for α_3 . In hypokalemic (1 mM) disease states, the fraction of enzyme in the species NEKK for α_1 , α_2 , and α_3 , respectively, is 66%, 64%, and 62%, and for NEK it is

15%, 14%, and 22%, respectively. This suggests that for all three isoforms, the pumping efficiency would be significantly lower in a hypokalemic state than in normal conditions, but there is very little difference among the three isoforms. The physiological significance of the increased affinity for Rb⁺ and decreased affinity for allosteric Na⁺ observed for the α_3 isoform is unclear.

The authors thank Dr. Carl L. Johnson and the late Dr. Shirley Bryant for helpful discussions.

This work was supported by National Institutes of Health grant RO1-HL50613.

REFERENCES

- Bell, M. V., F. Tondue, and J. R. Sargent. 1977. The activation of sodium-plus-potassium ion-dependent adenosine triphosphatase from marine teleost gills by univalent cations. *Biochem. J.* 163:185–187.
- Cavieser, J. D., and J. C. Ellory. 1975. Allosteric inhibition of the sodium pump by external sodium. *Nature*. 255:338–340.
- Cavieser, J. D., and I. M. Glynn. 1979. Sodium-sodium exchange through the sodium pump: the roles of ATP and ADP. *J. Physiol. (Lond.)*. 297:637–645.
- Forbush, B. 1987. Na, K, and Rb movements in a single turnover of the Na/K pump. *Curr. Top. Membr. Transp.* 28:19–39.
- Forbush, B. 1988. Rapid ⁸⁶Rb release from an occluded state of the Na, K-pump reflects the rate of dephosphorylation or dearsenylation. *J. Biol. Chem.* 263:7961–7969.
- Garrahan, P. J., and I. M. Glynn. 1967. The sensitivity of the sodium pump to external sodium. *J. Physiol. (Lond.)*. 192:175–188.
- Glynn, I. M. 1993. Annual review prize lecture. "All hands to the sodium pump." *J. Physiol. (Lond.)*. 462:1–30.
- Lentner, C. 1984. Geigy Scientific Tables, Vol. 3. Physical Composition of Blood. Hematology Somatometric Data. Medical Education Division, Ciba-Geigy, West Caldwell, NJ. 81–82.
- Lingrel, J. B., and T. Kuntzweiler. 1994. Na⁺,K⁺-ATPase. *J. Biol. Chem.* 269:19659–19662.
- Priestland, R. N., and R. Whittam. 1968. The influence of external sodium ions on the sodium pump in erythrocytes. *Biochem. J.* 109:369–374.

- Press, W. H., B. P. Flannery, S. A. Teukolsky, and W. T. Vetterling. 1986. Numerical Recipes: The Art of Scientific Computing. Cambridge University Press, Cambridge.
- Price, E. M., D. A. Rice, and J. B. Lingrel. 1989. Site-directed mutagenesis of a conserved, extracellular aspartic acid residue affects the ouabain sensitivity of sheep Na, K-ATPase. *J. Biol. Chem.* 264:21902–21906.
- Sachs, J. R. 1967. The competitive effects of some cations on active potassium transport in the human red blood cell. *J. Clin. Invest.* 46: 1433–1441.
- Sachs, J. R. 1977. Inhibition of the Na-K pump by external sodium. *J. Physiol. (Lond.)* 264:449–470.
- Sachs, J. R., and L. G. Welt. 1967. The concentration dependence of active potassium transport in the human red blood cell. *J. Clin. Invest.* 46: 65–76.
- Skou, J. D. 1957. The influence of some cations on and adenosine triphosphatase from peripheral nerves. *Biochim. Biophys. Acta.* 23:394–407.
- Squires, R. F. 1965. On the interactions of Na^+ , K^+ , Mg^{2+} and ATP with the Na^+ plus K^+ activated ATPase from the rat brain. *Biochem. Biophys. Res. Commun.* 19:27–32.
- Tepperman, K., L. A. Millette, C. L. Johnson, E. A. Jewell-Motz, J. B. Lingrel, and E. T. Wallick. 1997. Mutational analysis of glutamate 327 of Na, K-ATPase reveals stimulation of 86-Rb uptake by external potassium. *Am. J. Physiol. (Cell Physiol.)* 42:C2065–C2079.
- Yamamoto, S., T. A. Kuntzweiler, E. T. Wallick, N. Sperelakis, and A. Yatani. 1996. Amino acid substitutions in the rat Na^+ , K^+ -ATPase alpha 2-subunit alter the cation regulation of pump current expressed in HeLa cells. *J. Physiol. (Lond.)* 495:733–742.